MULTISPECTRAL IMAGING AS A TOOL FOR ENHANCING THE READING OF OSTRACA

Barak Sober, Shira Faigenbaum, Itzhaq Beit-Arieh, Israel Finkelstein, Murray Moinester, Eli Piasetzky and Arie Shaus

A recent study shows that multispectral (MS) imaging can improve the legibility of ostraca. Several examples of Iron Age ostraca unearthed over twenty years ago in Israel (Ḥorvat ʿUza and Ḥorvat Radum) are presented, showing how new images taken with an MS system improve the reading of inscriptions that have significantly faded over time. The article provides instructions for constructing a simple and low-cost MS imaging system that yields comparable results to commercial systems.[1]

1. INTRODUCTION

The vast majority of evidence of Hebrew writing from the Iron Age comes from ostraca (i.e., potsherds inscribed in ink; see, e.g., Davies 1991; Dobbs-Allsopp et al. 2005). These ink inscriptions are often found partially effaced and blurred. Furthermore, in uncontrolled, standard room conditions, the ink on the sherds fades more rapidly than it does when it is buried (Muros and Hirx 2004). Hence, in order to preserve and document, the ostraca, a procedure is needed to image them in advance of storage. The aim of this article is to redefine the standard protocol for ostraca imaging.[2]

Typically, a newly discovered inscription is imaged using a standard digital camera. In some cases, infrared (IR) imaging is used since, as is commonly argued, it improves the legibility of the inscription (e.g., Rosenbaum and Seger 1986; Zuckerman 1997; Bülow-Jacobsen 2008; Verhoeven 2008). In a recent study, our team showed that it is beneficial to use multispectral (MS) imaging techniques rather than standard photography or even IR imaging (Faigenbaum et al. 2012).

Since commercial MS imaging systems can be expensive and therefore out of range for some institutions, we have provided instructions (see Appendix A) for building a simple, low-cost MS imaging system that yields results comparable to commercial systems. All the images presented in this paper were produced using this low-cost system.

We will begin this paper by introducing some basic imaging concepts. We will then demonstrate ostraca image enhancement using MS imaging methods. Finally, we will present and discuss three cases in which the reading of ostraca changes as a result of using MS imaging techniques.

2. THE IMAGING PROCEDURE

2.1 Imaging in a nutshell

An image captured by a camera records the light reflected from objects in a scene. In other words, each point (pixel) in the image represents the light reflected from the corresponding

Address correspondence to: Barak Sober, Department of Applied Mathematics, Sackler Faculty of Exact Sciences, Tel Aviv University, Tel Aviv 69978, Israel. baraksov@post.tau.ac.il

point in space. This light can either belong to the visible light range (i.e., wavelengths of 350–750 nm; see Fig. 1) or be outside of it (e.g., IR – above 750 nm, ultra violet — under 350 nm).

A standard digital camera produces a Red, Green, and Blue (RGB) colour image. This image consists of three colour channels that correspond to different ranges of the visible light (red: 600–700 nm, green: 500–600 nm, blue: 400–550 nm).[3] By combining these channels, the viewer perceives a full-colour image. From the colour image, one can also create a grey level image by averaging the RGB channels. Additionally, each channel can be treated as a separate grey level image.

MS imaging produces a more detailed image than standard photography. Instead of three channels (ranges of wavelengths) representing red, green, and blue, the MS imaging typically produces eight, twenty, or even several hundred channels (depending on the spectral resolution, i.e., the wavelength range of each channel). The outcome of MS imaging is called *spectral cube* (see Fig. 2).

2.2 *The imaging procedure*

An experimental study (Faigenbaum et al. 2012) demonstrated that for each ostracon the optimal imaging wavelength is between 550 and 950 nm. Moreover, in order to capture the most favourable image, it is sufficient to use ten different band pass filters.

Accordingly, we used a standard digital camera that is sensitive to the visual spectrum (i.e., 400–700 nm). The internal IR cut filter was removed and replaced with transparent glass in

350 nm   750 nm

Fig. 1. The spectrum of visible light.
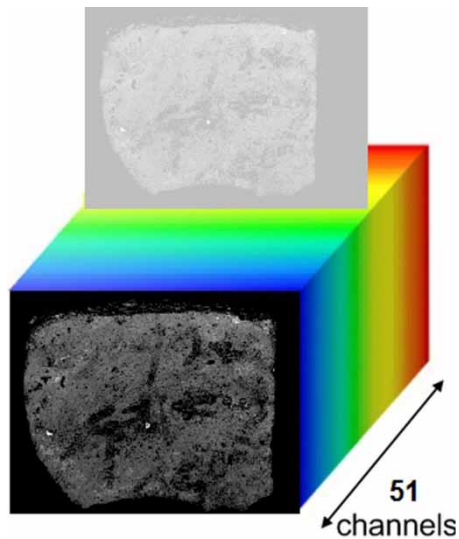

51 channels

Fig. 2. An illustration of a multispectral cube.

order to enhance the camera sensitivity in IR wavelengths (i.e., up to 1000 nm). Thereafter, the spectrum was sliced into ten channels utilising commercial external bandpass filters (for more details, see Appendix A).

Using this system, we produced a spectral cube of ten images for each ostracon. We selected the best image based on an algorithm that we developed (a short description of that algorithm is given in Appendix B).

In order to improve the legibility of the image, we performed contrast and brightness manipulations using image processing software. These manipulations can be performed using any of the available image processing software.

3. THREE EXAMPLES

In this section, we present three ostraca that were imaged using the MS procedure introduced above (Inscription No. 3 from Ḥorvat ʿUza and Inscriptions Nos. 1 and 2 from Ḥorvat Radum—both in the Negev; for the sites see Beit-Arieh 2007). A short description of the condition of each inscription adapted from the original excavation report is referred to below as *past state*. The *present state* of the ostracon (as observed by the naked eye) is specified as well. Next, the results achieved by the MS imaging technique are presented.

3.1 Inscription No. 3 (Reg. No. 2080/1) from Ḥorvat ʿUza

Past state: This ostracon was written on the outer surface of a jar sherd (8 × 5 cm). When it was unearthed and documented (Fig. 3, left), the inscription comprised eight fragmentary lines, and was identified as a list of names (Beit-Arieh 2007, 129–30).

Present state: The ostracon is faded. A significant number of the formerly discernible letters are not recognisable today (Fig. 4, left).

Using MS imaging: The eight lines and almost all of the letters are clear (Fig. 4, right). Moreover, in some cases, improvement is observed even with respect to the original image. For example, line 7, second letter on the right (enlarged in Fig. 5) was recognised as *yod* in the original publication of the inscription. After looking at the new image produced with our MS imaging system, it is recognised as ʾ*alep*.
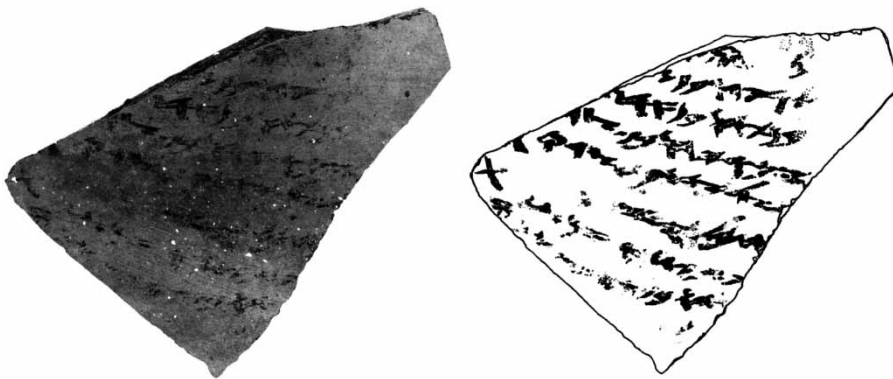

Fig. 3.   Inscription No. 3 from Ḥorvat ʿUza. Left — original image, photographed more than 20 years ago; right — the facsimile published in the excavation report (drawn by Ada Yardeni).
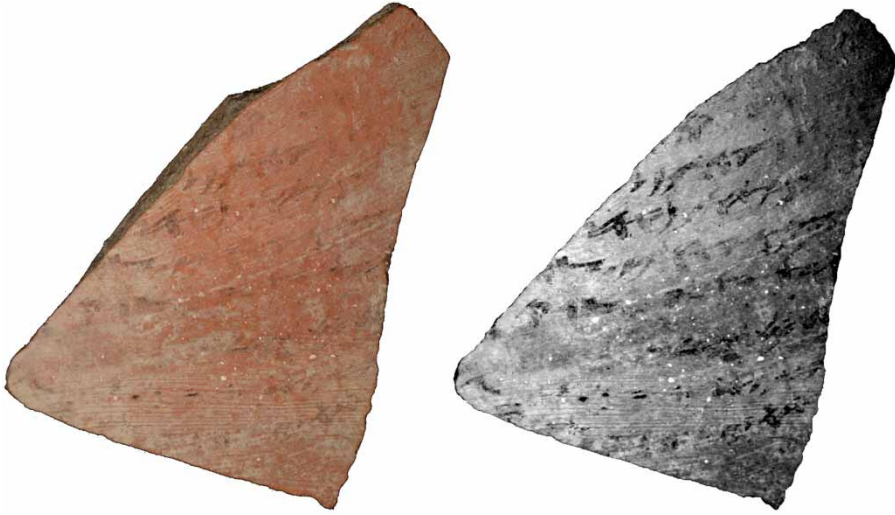
Fig. 4.   Images of Inscription No. 3 from Ḥorvat ʿUza. Left, new standard colour image; right, image photographed at wavelength 660 nm.
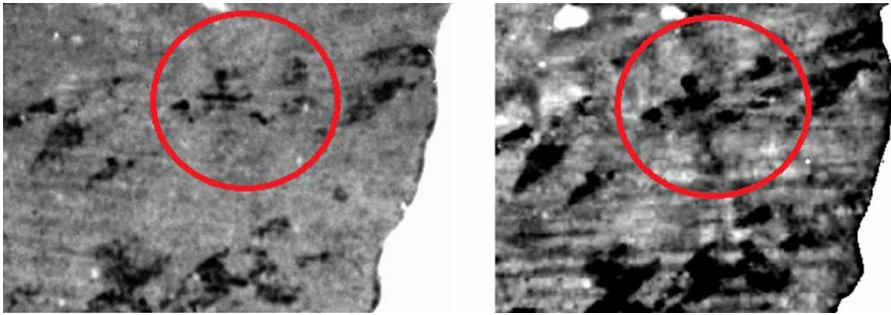

Fig. 5.   Images of Inscription No. 3 from Ḥorvat ʿUza zoomed in on the second letter on the right in line 7. Left, original image; right, image photographed at wavelength 660 nm.

Suggested transliteration:

I.	*-q*	ק-
2.	*-ryhw bn -*	-רי הובן-
3.	*-bnyhw bn ʾd*	-בניהובנאד-
4.	*zkryhw bn ṣd-*	-זכריהובנצד
5.	*-ṣlyhw bn sʔdq*	צליהובנצדק-
6.	*-ḥmly-*	-חמלי-
7.	*-ʾq-m-t*	-אק-מ-ת
8.	*- -hw bn-*	- הובן --

Fig. 6.   Inscription No. 1 from Ḥorvat Radum. Left, original image photographed more than 20 years ago; right, the facsimile published in the excavation report (drawn by Y. Kapelyan).

3.2 Inscription No. 1 (Reg. No. 4013) from Ḥorvat Radum

Past state: Four ostraca were found at Ḥorvat Radum and among them the only well preserved one is Inscription No. 1 (Beit-Arieh 2007, 323–24). The ostracon measures 3.8 × 5 cm and is written on the inner, burnished side of a bowl base. The inscription consists of three lines. Traces of a possible fourth line were found as well (Fig. 6).

Present state: The current condition of the ostracon is close to its condition immediately after excavation. Some degradation can be observed on the first line on the left side, and on the third line on the right side (Fig. 7, left).

Using MS imaging: The optimal MS image improves the overall legibility of the ostracon (Fig. 7, right). The degraded characters are visible again and even enhanced with respect to the image photographed 20 years ago. On line 2, the first character on the right was unrecognisable in the original image (see the facsimile in Fig, 6, right). In the image captured by the MS system, this character can be clearly recognised as the letter *kap* (Fig. 7, right). Moreover, another letter at the beginning of the third line (possibly *taw* or *kap*) can now be seen. This letter was not identifiable before.

Fig. 7.   Images of Inscription No. 1 from Ḥorvat Radum. Left, new standard colour image; right, image photographed at wavelength 635 nm.

Interpretation: The original reading of the inscription was "Ephron son of Elyaqim, servant". As the inscription seemed to be complete, it was understood as the name of a person and his title. The unidentified *kap* at the beginning of the second line was thought to be some sort of a geometrical design. The new evidence presented above rules out these suggestions. If the ostracon is indeed complete, it should now be read: "Ephron your son Elyaqim (?) servant", resulting in a less clear meaning than previously. Furthermore, the appearance of a new character at the beginning of the third line makes it even more challenging to interpret. We therefore speculate that this inscription is incomplete. Possible traces of a fourth line as well as traces of another character at the end of the second line support this view.

Original transliteration:

1.	ʾprn bn	‪-‬אפרן בן
2.	ʾlyqm	אליקם
3.	ʿbd	עבד

Suggested transliteration:

1.	ʾprn bn	‪-‬אפרנבנ
2.	k.ʾlyqm-	‪-‬כאליקם
3.	?.ʿbd	עבד.?

3.3 Inscription No. 2 (Reg. No. 4020/1) from Ḥorvat Radum

Past state: The ostracon measures *c.* 6.5 × 6.5 cm. The inscription is written on the inner side of the sherd and is encrusted by chalk that damaged the script (Beit-Arieh 2007, 324–25). Three lines can be discerned, but most of the letters are worn away. It is possible that the name Shallum appears on line 3 (Fig. 8).
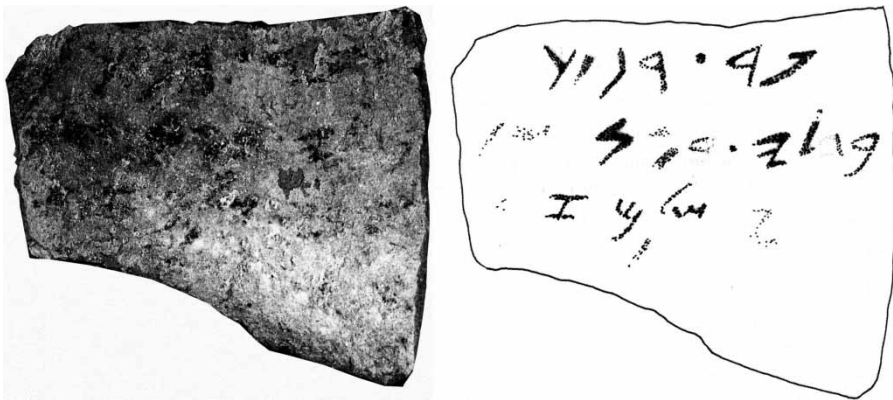

Fig. 8.   Inscription No. 1 from Ḥorvat Radum. Left, original image photographed more than 20 years ago; right, the facsimile published in the excavation report (drawn by Y. Kapelyan).
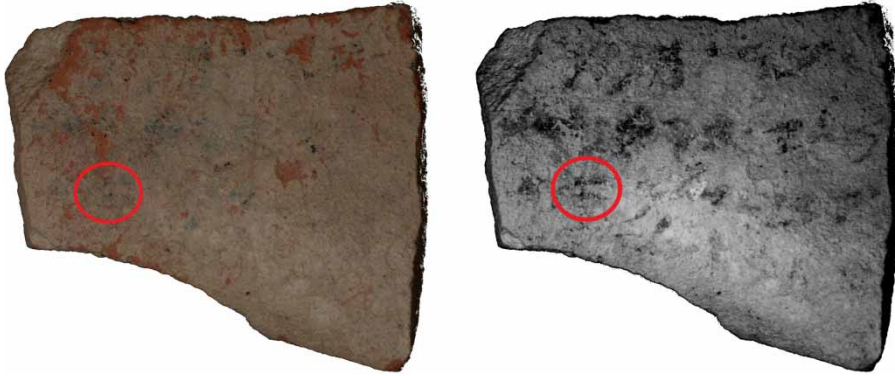
Fig. 9.   Images of Inscription No. 2 from Ḥorvat Radum. Left, new standard colour image; right, image photographed at wavelength 940 nm.
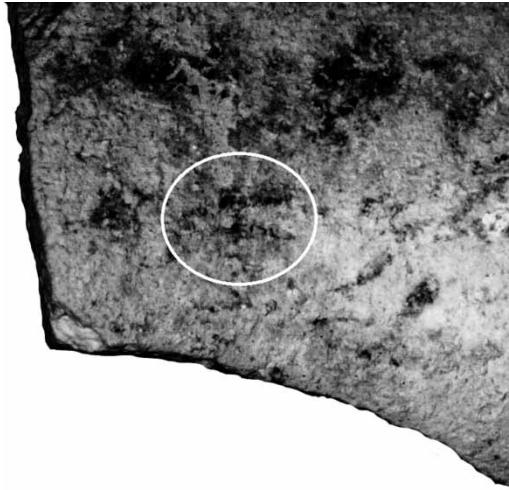

Fig. 10.   Image of Inscription No. 2 from Ḥorvat Radum zoomed in on the first letter after the name šlm in line 3.

Present state: It seems as if the chalk layer has grown thicker over the years and as a result the characters in this ostracon are barely legible. The three lines can still be discerned, but the name Shallum in the last line is no longer readable (see Fig. 9, left).

Using MS imaging: When imaging with IR light (wavelength 940 nm), the encrusted layer of chalk becomes transparent. The letters on line 3 reappear. Moreover, clear traces of a fourth line can be identified. The first character after the name *šlm* on the third line was originally recognised as *zayin* (see the facsimile in Fig. 8 right). In the new image produced with our MS imaging system it can be recognised as *ʾalep* (Fig. 10). On the fourth line, we can now discern several other letters which were not previously visible.

Original transliteration:

1.	*-pd.r—k*	כ--ר.פד
2.	*b-ly.- -n-*	נ- -.לי-ב-
3.	*- -šlm z-*	זמלש- - -

Suggested transliteration:

1.	*-pd.r—k*	כ- -ר.פד
2.	*b-ly.- -n-*	נ- -.לי-ב-
3.	*- -šlm .ʾ-*	א.מלש- - -
4.	- - - - - - - -	- - - - - - - -

4. CONCLUDING REMARKS

The above cases illustrate that MS imaging can improve ostraca documentation. The procedure enhances the legibility when compared to modern colour photography. Moreover, in the examples showcased above, the MS imaging compares favourably even with standard images taken shortly after the excavation, over twenty years ago. It is plausible that had this technique been used earlier, before the deterioration of the ostraca, additional epigraphic information would be available to us today.

The images presented above were produced using a low-cost MS system specifically designed for ostraca imaging. A high-cost commercial system[4] was used to image these ostraca as well and the results were almost identical (see Fig. 11).

The MS imaging method tested here on three ostraca found at Iron Age sites in Israel can be applicable to ostraca in general. It is also possible that this MS imaging can be useful in other cases where there is a need to enhance the contrast of ink over an opaque background (e.g., pottery decorations, rock paintings).

Fig. 11.   Images of Inscription No. 1 from Ḥorvat Radum. Left, image photographed using the low-cost system at wavelength 635 nm; right, image photographed with a high-cost commercial multispectral imager at wavelength 635 nm.

This research is part of a broader programme aimed at digitising and analysing Iron Age Hebrew ostraca, utilising computer science methodologies (Faigenbaum et al. 2012; Shaus, Finkelstein and Piasetzky 2010; Shaus, Turkel and Piasetzky 2012; Finkelstein et al. 2012). Producing better digital images of ostraca is the first phase of this project.

NOTES

[1] This article is dedicated to the memory of Prof. Itzhaq Beit-Arieh, who passed away on July 12, 2012.
[2] The question of optimal preservation conditions is beyond the scope of this paper.
[3] These channel wavelength ranges are no more than an approximation, and are different for each camera. More precise values of these ranges for our camera, Canon 450D, are given at: http://www.maxmax.com/ndvi_camera_technical.htm (last accessed: 15.07.2012).
[4] Nuance VariSpec SNIR-10 (short/near infrared) LCTF (liquid crystal tunable filter) multispectral imager.

APPENDIX A: THE LOW-COST IMAGING SYSTEM AND ITS MERITS

Faigenbaum et al. (2012) described a low-cost MS imaging system designed for imaging ostraca. The experimental study demonstrated that for each ostracon the optimal imaging wavelength lies somewhere between 550 and 950 nm. Moreover, in order to capture the most favourable image, it is sufficient to use ten different band pass filters.

Accordingly, we built a low-cost MS imaging system comprising a modified digital camera (IR cut filter removed) and a set of selected bandpass filters (see Fig. A1). This system can yield results comparable to a cutting-edge commercial system (Fig. 11, above).

To build this system, we used a Canon SLR 450D digital camera and a Tamron SP AF90 mm F/2.8 Di 1:1 macro lens. The internal Canon IR cut filter was removed by Lifepixel (web link [1]) and replaced with transparent glass having the same refractive index. The converted camera has useful quantum efficiency from about 400 to 1000 nm (web links [2, 3]), which follows from the characteristics of the CMOS imaging chip sensor. As a result, to achieve correct colour balance for normal (not IR) imaging, an external colour correction filter (we blink [4]) must be used.

An ideal set of filters for this imaging system would have transmission central wavelengths 525, 575, 625, 675, 725, 775, 825, 875, and 925 nm, each with 50 nm bandwidth. Since this choice is very expensive, we used ten 'off the shelf' filters instead. Six filters were produced by MidOpt (web link [5]). These have transmission centres at 525, 590, 635, 660, 695, and 735 nm. Two filters were produced by Omega (web link [6]), with transmission centres at 775 and 890 nm, and two by Maxmax (web link [4]), with transmission centres at 830 and 940 nm. All of the filters' bandwidths are 40 to 70 nm. Fig. A2 shows the coverage of the range 500–970 nm, using these ten filters.
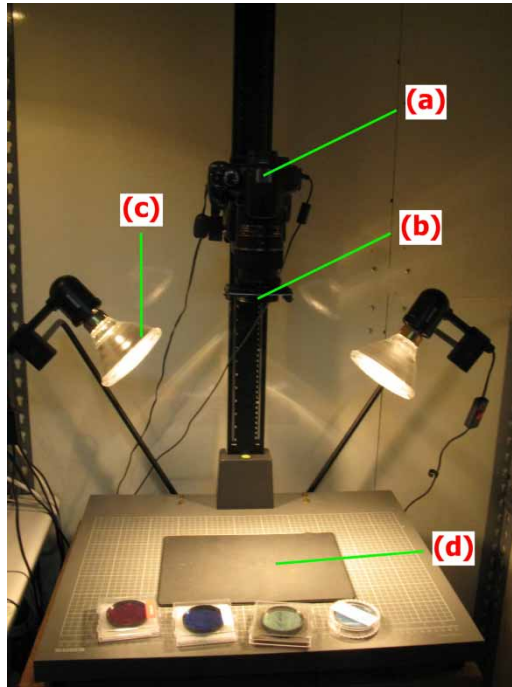
Fig. A1.   Image of the low cost MS imaging system. (a) Canon SLR 450D digital camera; (b) selected filter mounted over the macro lens; (c) 80W PAR38 Parabolic broad spectrum reflector lamps; (d) location of the ostracon.
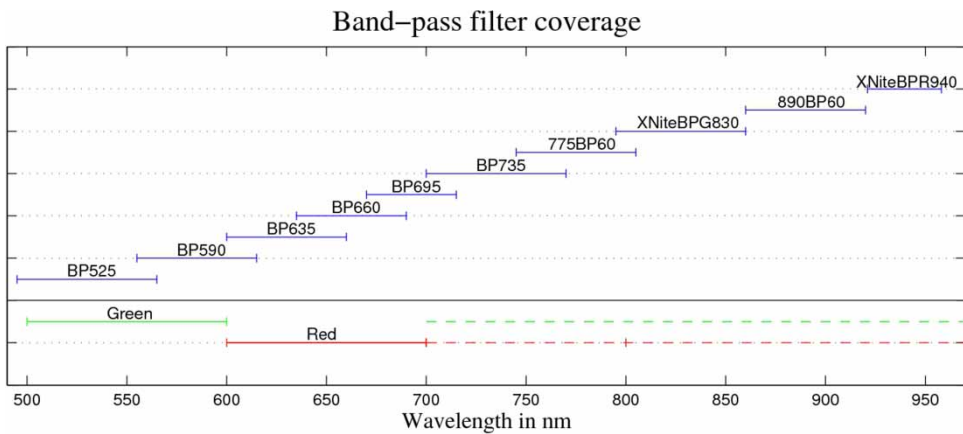

Fig. A2.   Above the vertical axis: off the shelf filters covering the complete range, each with a window of approximately 60 nm. Below the vertical axis: the sensitivity of the different channels in the camera (green and red, respectively). After removing the IR blocker, the sensitivity of the red and green channels extends up to 1000 nm, as shown by the dashed lines.

The procedure of imaging a given ostracon using the system described above is as follows:

- Place the ostracon on non-reflecting black background, to eliminate reflection.
- Mount the IR block filter to perform rough focusing.
- For each of the aforementioned filters:
  - Mount the filter.
  - As ostraca tend to have uneven surface, adjust the diaphragm smaller than maximum (using the f-stop function) to obtain greater depth of focus.
  - Set ISO to 100 since low values (of sensitivity) give lower background noise.
  - Adjust shutter speed to centre the grey level histogram of the red channel.
  - Focus using the camera's auto-focus function.
  - Take the image in RAW format and store it.
  - Repeat this process for the blue and green channels separately (optional).
- Select the best image either manually or by using the potential contrast measure (see Appendix B).
- Use image processing software (such as ImageJ, GIMP, and Adobe Photoshop) to enhance the brightness and contrast of the image.

APPENDIX B: POTENTIAL CONTRAST

Quality evaluation of an image can be carried out in many ways. Commonly used measures (such as Michelson, Weber, RMS) evaluate the contrast between foreground and background—ink and clay in our case (Peli 1990; Michelson 1927). However, these measures are
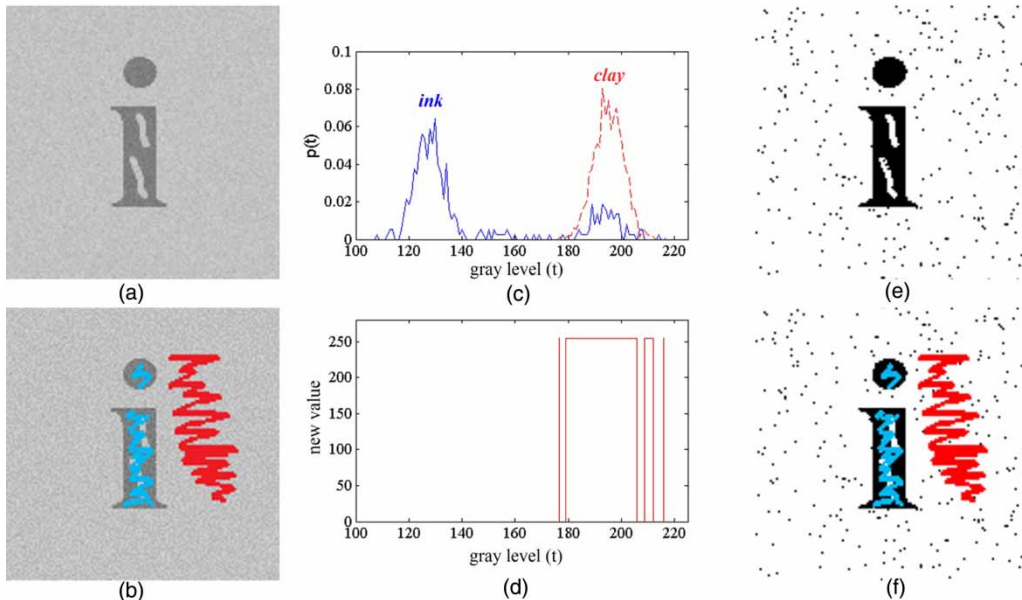

Fig. B1.   Applying the algorithm to an artificially constructed example: (a) the original image; (b) manually sampled areas: blue-foreground, red-background; (c) a plot of the two resulting grey level distributions: blue (solid)-foreground, red (dashed)-background; (d) setting each pixel value with either 255 or 0 according to and; (e) the output image after the pixel value changes (255 – white, 0 – black); (f) the sampled areas superimposed on the new image. In this example, PC(I) = 239.

themselves sensitive to standard manipulations (i.e., brightness and contrast transformations), performed using the available image processing software. A suggested solution to this problem uses the concept of *potential contrast*. The potential contrast of a given image provides a measure of the maximal contrast achievable by such manipulations. The image with the best potential contrast can then be selected out of a given set of images (in our case the spectral cube).

In order to calculate the potential contrast of an image, the following steps are performed (demonstrated in Fig. B1):

(i) Given an inscription image (Fig. B1a), areas of foreground (ink), and background (clay) are sampled manually (Fig. B1b).

(ii) The distributions of ink and clay grey levels, denoted respectively as $p_F(t)$ and $p_B(t)$, are derived using the sampled areas (Fig. B1c).

(iii) New values (255 or 0) are assigned to each pixel of the original image according to these distributions, in the following fashion:
- For a pixel with gray level t, if the probability for 'ink' is greater than (or equal to) the probability for 'clay' (i.e., $p_B(t) \leq p_F(t)$), its new value is 0.
- If, on the other hand, $p_B(t) > p_F(t)$, the pixel value is set to 255 (Fig. B1d).

This procedure produces a new black and white image (Fig. B1e).

(iv) The last step involves averaging the *new* values of the ink and clay sampled areas (Fig. B1f). Avg_F (Avg_B) denotes the average over the ink (clay) sampled pixels. By using these averages, the potential contrast (PC) is defined as:

$$PC(I) = Avg_B - Avg_F$$

For an ideal black and white picture, a pixel that belongs to the background (clay) is set to 255, while a foreground pixel (ink) is set to 0. Therefore, for such a picture, $PC = 255$.

In general, it can be proven that the PC represents the best achievable contrast of an image. Therefore, the 'potentially best' image is the one corresponding to the maximal PC value. For a more detailed mathematical discussion regarding the concept of potential contrast, see Faigenbaum et al. (2012).

ELECTRONIC SOURCES

[1] Lifepixel. Digital Infrared conversions (website): http://lifepixel.com. Last accessed: 15.07.2012.

[2] Maxmax. Canon 450D Xsi (website): http://www.maxmax.com/canon_450d_xsi.htm. Last accessed: 15.07.2012.

[3] Loop Technology. CMOS Sensor Cameras for Digital Vision. (website): http://www.loop technology.com/cmos-sensor-cameras.asp. Last accessed: 15.07.2012.

[4] Maxmax. 58 mm filters (website): http://www.maxmax.com/aXNite58mmFilters.asp. Last accessed: 15.07.2012.

[5] Midopt. Bandpass filters (website): http://www.midopt.com/filters.html. Last accessed: 15.07.2012.

[6] Omega optical. precision optical filters (website): http://www.omegafilters.com. Last accessed: 15.07.2012.

BIBLIOGRAPHY

Beit-Arieh, I., 2007. *Ḥorvat ʿUza and Ḥorvat Radum: Two Fortresses in the Biblical Negev*, Tel Aviv: Emery and Claire Yass Publications in Archaeology.

Bülow-Jacobsen, A., 2008. 'Infra-red imaging of ostraca and papryi', *Zeitschrift für Papyrologie und Epigraphik* 165, 175–85.

Davies, G. I. (ed.), 1991. *Ancient Hebrew Inscriptions: Corpus and Concordance*, Cambridge: Cambridge University Press.

Dobbs-Allsopp, F. W., et al., 2005. *Hebrew Inscriptions: Texts from the Biblical Period of the Monarchy With Concordance*, Connecticut: Yale University Press.

Faigenbaum, S., et al., 2012. 'Multispectral images of ostraca: acquisition and analysis', *Journal of Archaeological Science* 39–12, 3581–90.

Finkelstein, I., et al., 2012. 'Reconstructing ancient Israel: integrating macro- and micro-archaeology', *Hebrew Bible and Ancient Israel* 1, 133–50.

Michelson, A. A., 1927. *Studies in Optics*, Chicago: University of Chicago Press.

Muros, V., and Hirx, J., 2004. 'The use of Cyclododecane as a temporary barrier for water-sensitive ink on archaeological ceramics during desalination', *Journal of the American Institute for Conservation* 43, 75–89.

Peli, E., 1990. 'Contrast in complex images', *Journal of the Optical Society of America A* 7, 2032–40.

Rosenbaum, J., and Seger, J. D., 1986. 'Three unpublished ostraca from Gezer', *BASOR* 264, 51–60.

Shaus, A., Finkelstein, I., and Piasetzky, E., 2010. 'Avoiding the eye of the beholder: automated ostraca facsimile evaluation', *Maarav* 17, 7–20.

Shaus, A., Turkel, E., and Piasetzky, E., 2012. 'Quality evaluation of facsimiles of Hebrew First Temple period inscriptions', *10th IAPR International Workshop on Document Analysis Systems*, 170–74.

Verhoeven, G., 2008. 'Imaging the invisible using modified digital still cameras for straightforward and low-cost archaeological near-infrared photography', *Journal of Archaeological Science*, 35, 3087–100.

Zuckerman, B., 1997. 'Photography of manuscripts', in E. M. Meyers (Ed.), *Oxford Encyclopedia of Archaeology in the Near East, 4*, Oxford: Oxford University Press, 336–47.